HHS Public Access

Author manuscript

Exp Cell Res. Author manuscript; available in PMC 2019 November 01.

Published in final edited form as:

Exp Cell Res. 2018 November 01; 372(1): 73–82. doi:10.1016/j.yexcr.2018.09.014.

L-Plastin Phosphorylation Regulates the Early Phase of Sealing Ring Formation by Actin Bundling Process in Mouse Osteoclasts

Meenakshi A. Chellaiah[*], **Tao Ma**, and **Sunipa Majumdar**

Department of Oncology and Diagnostic Sciences Dental School, University of Maryland, Baltimore, Maryland

Abstract

The process of sealing ring formation requires major actin filament reorganization. We previously demonstrated that an actin-bundling protein L-plastin has a role in the cross-linking of actin filaments into tight bundles and forms actin aggregates (denoted as nascent sealing zones). These nascent sealing zones mature into fully functional sealing rings. We have shown here that TNF-alpha signaling regulates the phosphorylation of serine-5 and −7 in L-plastin which increases the actin bundling capacity of L-plastin and hence the formation of nascent sealing zones in mouse osteoclasts. Using the TAT-mediated transduction method, we confirmed the role of L-plastin in nascent sealing zones formation at the early phase of the sealing ring assembly. Transduction of TAT-fused full-length L-plastin peptide significantly increases the number of nascent sealing zones and therefore sealing rings. But, transduction of amino-terminal L-plastin peptides consisting of the serine-5 and −7 reduces the formation of both nascent sealing zones and sealing rings. Therefore, bone resorption in vitro was reduced considerably. The decrease was associated with the selective inhibition of cellular L-plastin phosphorylation by the transduced peptides. Neither the formation of podosomes nor the migration was affected in these osteoclasts.

Phosphorylation of L- plastin on serine 5 and −7 residues increases the F-actin bundling capacity. The significance of our studies stands on laying the groundwork for a better understanding of L-plastin as a potential regulator at the early phase of sealing ring formation and could be a new therapeutic target to treat bone loss

Graphic Abstract

[*]Correspondence: Meenakshi A. Chellaiah PhD, Department of Oncology and Diagnostic Sciences, Dental School, University of Maryland, Baltimore, MD 21201, Tel.: (410) 706-2083, fax: (410) 706-6115, mchellaiah@umaryland.edu.

Authors' Contributions: TM and SM designed and generated full length, deletion and mutant constructs of LPL; MAC conceived, designed, and performed the experiments; MAC analyzed the data and wrote the paper.

Disclosures

All authors declare that they have no conflicts of interest.

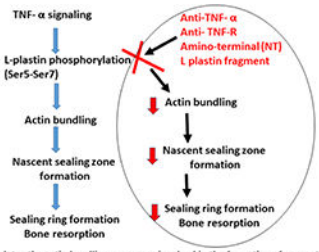

Phosphorylation of L-plastin regulates the actin bundling processes involved in the formation of nascent sealing zones (NSZs) which are considered as a precursor zones for the mature sealing rings. These NSZs mature into fully functional sealing rings in a time dependent manner by the signaling mechanisms mediated by integrin αvβ3. Inhibiton of phosphorylation of L-plastin by the indicated inhibitors in the red circle, attenuates not only the formation of NSZs but also the fully functional sealing rings; hence these osteoclasts display reduced bone resorption. Inhibition is indicated by red arrows.

Keywords

Osteoclasts; cytoskeleton; L-Plastin; nascent sealing zones; sealing rings; bone resorption

Introduction

Several actin-binding proteins are involved in the cytoskeletal organization during cell migration, invasion, adhesion, and bone resorption. Our previous observations in gelsolin null (Gsn−/−) osteoclasts demonstrated that gelsolin deficiency blocks podosome assembly and motility. However, these cells still exhibit sealing ring and matrix resorption [9]. Therefore, Gsn−/− osteoclasts are capable of resorbing bone, but the resorbed areas are small due to the absence of podosomes and the resulting hypo-motile nature of osteoclasts [9]. Observations in Gsn−/− osteoclasts also suggest that the organization of sealing ring presumably reflects changes in the role of actin-binding proteins. Sealing ring formation in osteoclast is a requirement for bone resorption. Due to the architectural nature of sealing rings, the major reorganization of actin filaments is required during their formation. Knowledge of the formation of mature sealing rings remains limited. Sealing rings consisting of actin filaments that generate tight sealing zones on the bone surface during bone resorption by osteoclasts. Spatial configurations of actin filaments by actin-binding/bundling proteins (ABPs) account for the specific cytoskeletal changes during bone resorption.

We have previously shown that cyclical changes in protein and phosphorylation levels of Lplastin (LPL) and cortactin correspond with time-dependent changes in actin organization in osteoclasts subjected to bone resorption. We were the first to have shown the assembly of actin aggregates at the early stage of sealing ring formation by TNF-alpha (TNF-α) or RANKL signaling independent of integrin αvβ3 signaling. These actin aggregates are denoted as nascent sealing zones (NSZs) [40]. These NSZs function as a central point or a hub in assembling molecular components (integrin αvβ3, Src, cortactin, ERK, WASP, and Arp2/3) involved in the maturation of NSZs to fully functional mature sealing rings [11, 12, 40, 41]. Timedependent changes in the localization of LPL in NSZs and cortactin in sealing rings suggest that these proteins may be involved in the initial and maturation phases of sealing rings, respectively. Although integrin signaling has been shown to play a role in the formation of the sealing rings, its role in the maturation of NSZs to sealing rings has not yet been studied

TNF-α was shown to stimulate the resorptive activity of osteoclasts independently of αvβ3 [22, 23]. The definite target of TNF-α signaling has not been identified. Lysates made from osteoclasts treated with native mice bone particles (60–80μm size) and TNF-α or RANKL revealed a possible mechanistic role in the organization of NSZs by LPL. Time-dependent localization of LPL in NSZs suggests a role for this protein in the formation of stable actin filaments and localization of integrin αvβ3 in these zones. NSZs are converted to ring-like configurations at which time localization of LPL is reduced. Treatment of osteoclasts with αv inhibitor did not affect the formation of NSZs and localization of integrin in NSZs. However, localization of Src and cortactin in NSZs and maturation of NSZs to fully functional sealing rings are blocked [40].

LPL is present predominantly in hematopoietic cells (e.g. lymphocytes, neutrophils, and T-cells and osteoclasts) [21, 27, 40]. It is also known as Plastin 2, cytoskeletal associated protein (CAP) or fimbrin [3, 14, 44, 59]. LPL is capable of distinguishing between actin isoforms, and has been shown to bundle β-actin efficiently but not α- actin or G-actin [49]. The aminoterminal (N-terminal) domain of LPL contains two phosphoserine residues (Ser-5 and Ser-7), Ca2+binding sites flanked by EF-hand motifs, two repeated actin-binding domains (ABDs) and calponin homology domain (CH) at the carboxyl-terminal end. The spatial proximity of ABDs (120Å) of LPL enable them to organize actin filaments into tight bundles [2, 6]. LPL localizes to actin-rich membrane structures involved in locomotion, adhesion, and membrane extensions (e.g. filopodia, lamellipodia) [3, 13, 28, 66]. Phosphorylation of LPL on residues Ser-5 and −7 occurs in hematopoietic cells [15, 53] but most likely on Ser-5 exclusively in non-hematopoietic cells.

How spatial and temporal localization of actin-modulating protein(s) and actin control the formation of sealing ring still needs further elucidation. We believe that sealing rings required bundled actin filaments to generate tight sealing zones for active bone resorption to occur. While many of the proteins that compose the sealing ring have been identified, their function is still poorly understood. The knowledge of the formation of NSZs before mature sealing ring development is very limited. We are the first ones to show LPL as a novel target for TNF -α signaling which provided a new perspective at the early phase of sealing ring formation [40].

Here, our principal goal was first to characterize the elements of LPL involved in the actin bundling process at the early phase of sealing ring organization in osteoclasts. We have previously demonstrated that the transduction of TAT-fused full-length peptides of constitutively active (V14-Rho)/ dominant negative (N19-Rho) Rho, gelsolin, and WASP protein as well as different domains of gelsolin and WASP resulted in dramatic changes in the migratory and resorptive potential of osteoclasts [5, 10, 39, 41, 61]. TAT-WASP and TAT-CD44 peptides against phosphodomain of the corresponding proteins demonstrated significant inhibitory effects on the invasion and migration of prostate cancer cells (PC3) derived from bone metastasis [16, 17]. TAT-fused proteins of different molecular weight revealed the potential to enter into the cell type of interest and displayed specific biological activities in an efficient manner.

In this paper, we have used similar structure-function analyses to determine the domains of LPL which has a key role in the actin bundling process. We cloned full length (FL-LPL) and mutated full length (Ser-5 and Ser-7 to Ala-5 and Ala-7) as well as amino-terminal LPL (NT-LPL) and actin-binding domains of LPL (ABD-LPL) in a TAT expression vector containing hemagglutinin tag (HA). TAT fused proteins were purified [10, 61] and transduced into mouse osteoclasts. The effects of these proteins on the phosphorylation of endogenous or cellular LPL, NSZ and sealing ring formation, bone resorption, and migration were determined. A significant decrease in the phosphorylation of cellular LPL and NSZ formation was observed in osteoclasts transduced with NT-LPL which suggest that LPL phosphorylation on Ser-5 and Ser-7 residues is critical for actin bundling activity of LPL.

Materials and Methods

Antibody to LPL (SC-16657; Goat) was bought from Santa Cruz Biotechnology, Inc. (Santa Cruz, CA). Antibodies to GAPDH and TNF-α receptor 1 (TNFR1) were purchased from R & D Systems (Minneapolis, MN). Protein estimation reagent, molecular weight standards for proteins, and PAGE reagents were bought from Bio-Rad (Hercules, CA). Molecular weight markers have also been bought from Promega (Madison, WI). Cy2- and Cy3-conjugated secondary antibodies were purchased from Jackson Immunoresearch (West Grove, PA). HRPconjugated secondary antibodies for immunoblotting and phosphoserine (p-Serine) antibody were bought from Abcam (Cambridge, MA). Mounting solutions for mounting of coverslips were bought from Thomas Scientific (Swedesboro, NJ) or Vector Labs (Burlingame, CA). Rhodaminephalloidin and all other chemicals were purchased from Sigma (St. Louis, MO).

Mice

C57/BL6 mice (six to eight-week-old mice) were used for osteoclast preparation. These mice were either purchased from Harlan Laboratories or generated in the animal facility of the University of Maryland Dental School. Breeding and maintenance were carried out as per the guidelines and approval of the institutional animal care and use committee

Preparation of osteoclasts from long bones of Mice

Osteoclasts were generated in vitro using long bone marrow cells of six to eight-weeks-old C57BL/6 mice as described previously [9, 11]. The multinucleated osteoclasts were seen from day four onward. There are limitations in obtaining homogenous multinucleated osteoclasts from the bone marrow macrophages of the long bones of mice. However, the heterogeneous culture consists of a large number of (>85%) multinucleated giant osteoclasts and some osteoclast precursors (~10 to 15%).

Treatment of osteoclasts with bone particles and TNFR-1 antibody

Bone particles (60–80 μm in size) were prepared as described previously [40]. After flushing the marrow cells for osteoclast differentiation as described above, long bones of mice (free of cells inside and muscles outside) were washed extensively with PBS and kept in ethanol until use. Long bones were air-dried in the hood and homogenized by a mini blender. Bone particles were sieved and used for experiments. Multinucleated osteoclasts were seen from

day four onward. At this time cultures were added with bone particles (100μg/ml media) for 3–4 h or 12–14h in the presence of TNF-α (20ng/ml). Some cultures were treated with 3–5μg/ml TNFR1 antibody. Osteoclasts were preincubated with the TNFR1 antibody for 60–90 min before the addition of TNF-α to enhance the blocking effect. Osteoclasts incubated with bone particles for 3–4 or 12–14 h in the presence of TNF-α were used for lysate preparations.

Cloning of L-Plastin constructs

Bacterial expression constructs coding various HIV-TAT fusion peptides of LPL were generated by PCR method as described [41]. LPL constructs were generated from mouse cDNA library using the following primers: Full length (FL-) LPL: (F) 5'- ACA TGA CCG GTA TGG CCA GAG GAT CCG TG −3' and (R) 5'- CAC ATG AAT TCA CTT ACA CCC TCT TCA TCC CTT TC – 3'; Amino terminal (NT)-LPL: (F) 5'-ACA TGA CCG GTA TGG CCA GAG GAT CCG TG −3' and (R) 5'- CAC ATG AAT TCA CTT AGT ACC CAG GCA GAG GCA GGC AG −3'; Actin binding domain (ABD) of LPL: (F): 5'- ACA TGA CCG GTA CCT CTG AGC AGT CCA GCG TTG −3' and (R) 5'- CAC ATG AAT TCA CTT ACT TCT GTC CAC CTC CGA TAT C −3'. The PCR products of LPL were inserted into the Age1/EcoR1 site of a bacterial expression vector, pTAT-HA, to produce TAT fusion proteins. The sequences of all the clones were confirmed for reading frame by DNA sequencing.

Site-directed mutagenesis of L-plastin

Mutations at Ser-5 and Ser-7 were generated using the Quick Change Site-Directed Mutagenesis (SDM) Kit (Agilent Technologies, Halethorpe) and as per the instructions provided in the manufacturer's protocol. Full- length LPL (FL-LPL) cDNA (Accession: BC010271) have been used to generate the Ser-5 and Ser-7 to Ala-5 and Ala-7 mutant. The following forward and reverse primers with Sal1 and Sph1 sites, respectively are used to generate the mutants: F5'-ACGCGTCGACATGGCCAGAGGAGCAGTGGCCGATGAGGAAATGATGGAG-3';R5'–TGCTG CAGCATGCATTCTGCCCTC 3'. First, the Sal1-Sph1 fragment of the mutated cDNA was generated in pCMV-SPORT6. Several positive clones have been identified and sequenced at the University of Maryland Core Facility to verify the insertion of expected mutations and also for the insertion of any other unsought mutations during the mutagenesis process. Subsequently, mutated FL-LPL was cloned into the pTAT-HA vector at Kpn1-EcoR1 sites to produce mutated TAT-fused mutated FL-LPL protein. The forward and reverse primers containing Kpn1-EcoR1 sites, respectively are as follows: F-'5' CGGGGTACCATGGCCAGAGGAGCAGTGGCC-3';R-5'GGAATGAAGAG GGTGTGAGAATT CCGG-3'.

Vector pTAT-HA and Purification of TAT-fused LPL proteins

We used pTAT-HA expression vector for cloning and purification of the indicated L-plastin constructs. pTAT-expression vector was kindly provided by Dr. Steven Dowdy Professor of Cellular and Molecular Medicine; University of California San Diego; School of Medicine) [47]. The vector pTAT-HA has N-terminal 6-histidine leader, TAT protein transduction domain (11amino acids) flanked by glycine residues, a hemagglutinin (HA) tag, and

polylinker. HSV-TK (Herpes simplex virus thymidine kinase; 42kDa) protein was used as a control. The purification protocol is adapted from the published procedure using a Ni-NTA column [10, 47, 61]. The fusion protein is expressed in BL-6 bacteria and then isolated by using Ni-NTA column. Briefly, bacterial pellets were resuspended in a buffer containing 100 mM NaCl, 20 mM Hepes (pH 8.0), and 8 M urea, sonicated, and centrifuged at 12,000 rpm for 10 min at 4 °C. Imidazole was added to the supernatant to a final concentration of 10–20 mM and purified in Ni-NTA column as described [10, 61]. Addition of 8 M urea to the sonication buffer allows for the isolation of insoluble proteins in bacterial inclusion bodies and efficient transduction into cells. Bound proteins were eluted with stepwise addition of 5–10 ml each of 100, 250, and 500 mM and 1 M imidazole in the above buffer. Rapid dialysis removed urea by using the Slide-A-Lyzer cassette (Pierce Chemical Co.) or by the use of desalting PD-10 columns (Sephadex G-25) (Amersham Pharmacia Biotech). Desalting was done per the manufacturer's instructions. Protein transduction technology offered a way to purify misfolded TAT-HA fused recombinant fusion proteins of interest. These proteins are highly insoluble in the inclusion bodies of the bacteria. Partial unfolding of the protein enhances the ability of the recombinant protein to enter into cells of interest [47]. Purification protocol with urea assist in the mis-or unfolding of TAT-fusion proteins; once transduced into cells, these proteins may be refolded by the chaperones [e.g. HSP90] [52].

Transduction of TAT-fused LPL proteins into osteoclasts

For transduction with TAT-fused peptides (100–150nM), osteoclasts were first kept in serum-free α-MEM for two h. Afterward, TAT proteins of interest, bone particles, and TNF-α were added to cells in serum-free α-MEM. Lysates were made from these cells for immunoprecipitation and immunoblotting analyses. Osteoclasts plated on dentine slices in the presence of TAT-proteins of interest and TNF-α for 3–6h or 10–12h were used for immunostaining or actin staining analyses. Osteoclast cultures treated only with TNF-α were used as controls.

Lysate preparation, Immunoprecipitation and Immunoblotting analysis

Following various treatments, osteoclasts were washed three times with cold PBS and lysed in a radioimmune precipitation buffer (RIPA; 10 mM Tris-HCl, pH 7.2, 150 mM NaCl, 1% deoxycholate, 1% Triton X-100, 0.1% SDS, 1% aprotinin, 2mM PMSF, 100 M Na_3VO_4, and 1% aprotinin). Cells were rocked on ice for 15 min and scraped off with a cell scraper. Cell lysates were centrifuged at 15,000 rpm for 5 min at 4 °C, and the supernatant was saved. Protein contents were measured using the Bio-Rad protein assay reagent. Equal amounts of lysate proteins (100–150μg) were used for immunoprecipitations. Immunoprecipitations and Western blotting were done as described previously [7,8].

Fluorescent labeling of proteins in osteoclasts

Osteoclast precursors (10^5 cells/coverslips) were cultured on glass coverslips or dentine slices. Fluorescent labeling was done in osteoclasts transduced or untransduced with TAT-proteins. HA or TAT antibody was used to identify the transduced peptides of interest; rhodamine phalloidin was used to determine actin organization [9, 10]. L-plastin antibody was used to determine the distribution of LPL in a time-dependent manner as shown previously [40]. Immunostained and actin stained osteoclasts were photographed with a Bio-

Rad confocal laserscanning microscope. Images were stored in TIF image format and processed by Adobe Photoshop (Adobe Systems Inc., Mountain View, CA).

Measurement of filamentous actin (F-actin) content with rhodamine phalloidin

For the measurement of F-actin, osteoclasts transduced with TAT-LPL peptides of interest for 15 to 30min. were replated on dentine slices for 3 to 4h or 10–12h, respectively, in the presence of indicated TAT-fused peptides of interest and TNF-α. For each treatment four to six wells in 24 well, culture dishes were used. Cells were fixed and rhodamine phalloidin binding to F-actin was done as described [9, 10].

Resorption pit formation assay in vitro using dentine slices

Osteoclasts transduced with TAT-LPL peptides of interest for 30min. were replated on dentine slices for 10–12 h in the presence of TAT-fused peptides of interest and TNF-α. Some cultures were treated with a neutralizing antibody to TNFR-1. Resorption assay was performed as described previously [9, 10]. Resorbed areas were also scanned in confocal microscopy. Images were stored in TIF format and processed by Adobe Photoshop (Adobe Systems Inc.) [9]. The resorbed pit areas were quantified and data were compiled from four slices per treatment and per experiment. The resorbed pit areas (20–25 pits/slice) were quantified and data were compiled from four slices per treatment. The data showed is the mean ± SEM of one experiment performed. The area of the pit was determined from the free-hand traced perimeter using the LSM software [9]. As per Cosmo Bio recommendations, we compiled the results of one experiment for the presentation.

Transwell migration assay

Transwell migration was done as reported previously [9]. Osteoclasts that migrated to the underside of the transwell membrane were stained with hematoxylin stain. Dried filters were cut out and mounted with a permount solution (Thomas Scientific, Swedesboro, NJ) on a glass slide. Cells were viewed under X40 objective in an inverted microscope. Six fields per transwell insert were counted using a Zeiss microscope as described previously [10]. Data are presented as the number of cells per migrated field (mean ± SD) from one experiment.

Statistical Analysis

Data obtained represent the response of the osteoclast culture as a whole (>85% multinucleated giant cells and ~10–15% osteoclast precursors). Statistical significance was determined using either analysis of variance ANOVA or student's t-Test (INSTAT; Version 6.0, Graph Pad software, Graph Pad Inc., San Diego, CA). The data are depicted as the mean ± SD or the mean ± SEM. A probability value *$p < 0.05$ was considered statistically significant (*, $p<0.05$; **, $p<0.01$; ***, $p<0.001$).

Results

Expression and purification of the TAT-fused LPL peptides

The following HA- TAT fused LPL proteins were generated: unmutated (FL-LPL) and mutated (FL-LPL (A5A7)) full-length LPL (~80kDa), amino terminal (NT)-LPL-15kDa),

and actin binding domains (ABD; 50–55kDa) of LPL (Figure 1A). Purified proteins were analyzed in an 8% (FLLPL; ABD-LPL) or 15% (NT-LPL and TAT-HA vector protein) SDS-PAGE. Gels were stained with Coomassie blue stain (Figure 1B). TAT-HA vector (8–10 kDa) and Herplex Simplex Virus thymidine kinase (HSV-TK; 42 kDa) proteins were used as controls for transduction experiments [10]. Small molecular weight proteins are (<10kDa) are very difficult to separate on a SDSPAGE. These proteins migrate with the dye and buffer front. TAT-HA vector protein always run larger than the expected size with ~MW between 8 and 10kDa. We consistently see this difference [5, 10, 41, 61]. Usage of different sample buffer did not change the size of the protein. We believe that it may be due to the property of the purified vector protein. NT-LPL peptide has the first 45aa sequences of LPL. Theoritical pI/MW is 4.21/4886.47dalton; as a fusion protein with vector sequences, it provided the MW ~15 kDa on the SDS-PAGE. Similarly, a small increase in the size of FL-LPL and ABD-LPL was observed (Figure 1B).

Dose- and time-dependent uptake of proteins by osteoclasts were done as shown previously [10]. Maximum uptake was seen between the 100–200nM dose of TAT-fused FL-LPL (Figure 1 C; lanes 3–5). The uptake of TAT-fused FL-LPL reaches maximal levels at 45 min to 2h (Figure 1 D; lanes 4 and 5) and the protein appeared to be stable for up to 6–8h (lane 6) and reduced from 12h onwards (lanes 7–9). Therefore, osteoclasts were incubated with 150nM TAT-fused peptides (control and LPL peptides) for 3–4h. Loading was normalized to the cellular levels of GAPDH for blots shown in C and D. Based on these experiments, 100–150nM concentration of TAT proteins have been used for experiments shown below.

Analysis of the effect of transduction of TAT-fused LPL peptides on the phosphorylation of endogenous LPL

Previous studies, including our own have shown that the actin bundling process is dependent on the phosphorylation of LPL [1, 15, 40, 46, 64]. Here, we aim to elucidate the significance of LPL phosphorylation on actin dynamics associated with the NSZs formation in osteoclasts transduced with TAT-fused LPL peptides (Fig. 1). We first examined the phosphorylation of endogenous LPL in the presence of bone particles and TNF-α. Osteoclasts untransduced (Fig. 2A; lane 1) or transduced with peptides such as unmutated (lanes 2 and 5) and mutated FL-LPL (lane 6), ABD (lane 4) and non-specific control peptide HSV-TK (lane 7) demonstrated basal level phosphorylation of endogenous LPL (~68–70kDa). Phosphorylation of the transduced TATfused FL-LPL was also seen at a molecular mass of ~80kDa in FL-LPL transduced osteoclasts (Fig.2A; lanes 2 and 5) and not in mutated FL-LPL transduced osteoclasts (lane 6). Most importantly, transduction of NT-LPL exerted a significant inhibitory effect on the phosphorylation of endogenous LPL (lane 3). Inhibition was found to be >72 ± 7.3% (mean ± SD of three blots) with NT-LPL peptide. Immunoblotting with an LPL antibody demonstrates both endogenous LPL protein (Fig. 2B, Lanes 1–7) and transduced FL-LPL peptide (mutated and unmutated; lanes 2, 5, and 6).

We proceeded to determine whether the decrease in the phosphorylation of cellular LPL (Fig. 2A, lane 3) is due to competitive inhibition mediated by the transduced NT-LPL peptide. Immunoblotting with a p-Serine antibody (Fig. 2D; lanes 1 and 2) demonstrated the phosphorylation of transduced NT-LPL peptide (Fig. 2D; lane 2). Stripping and reprobing of

this blot with an antibody to HA demonstrate the immunoprecipitated levels of the transduced NTLPL level (Figure 2D, lane 4). Neither NT-LPL nor phospho-NT-LPL was observed in the immunoprecipitates made with non-immune serum (NI; Fig. 2D; lanes 1 and 3). GAPDH immunoblot was used to normalize the amount of lysate protein used (input) for indicated immunoprecipitations (Panels C and D). Results with mutated FL-LPL (A5A7) and NT-LPL suggest that TNF-α signaling regulates the phosphorylation of LPL protein. Also, NT-LPL peptide can inhibit the phosphorylation of endogenous (cellular) LPL competitively.

Analysis of the effect of transduction of TAT-fused LPL peptides on NSZs formation in osteoclasts plated on dentine

We performed confocal analyses in mouse osteoclasts plated on dentine slices for 3–4h and 6–8h and immunostained with an antibody to LPL and stained with rhodamine phalloidin for actin (Figure S1). Consistent with our previous observations [40], LPL is colocalized with actin in the NSZs of osteoclasts plated on dentine slices for 3–4h (indicated by white arrows; Figure S1A). Colocalization of LPL and actin was not observed in the mature sealing rings of osteoclasts plated on dentine for 6–8h (indicated by a white arrowhead). This corroborate our previously published data on the time-dependent localization of LPL in the NSZs of osteoclasts plated on dentine slices [40]. Consequently, it was of interest to study whether the transduced peptides would modulate actin dynamics in osteoclasts and whether this modulation was associated with the phosphorylation of transduced peptides. Therefore, osteoclasts transduced with various domains of LPL were plated on dentine slices for 3–4h in the presence of TNF-α and actin staining was done (Fig. 3, A-F). The number of NSZs were counted in ~75 osteoclasts and provided as a graph (Fig. 3G). We also examined the effects of various TAT-fused LPL peptides on the total F-actin content of osteoclasts (Figure 3H). Actin staining showed that NSZs were found at the extensions of the plasma membrane. The number of NSZs and F-actin content are more or less equal in osteoclasts transduced with peptides such as HSV-TK, mutated FL-LPL (A5A7), and ABD-LPL (Fig. 3A, B, and E). ABD alone had no effect on the actin bundling process and NSZs formation. The level observed in these osteoclasts are considered the basal level and no additional actin bundling process took place. However, a substantial increase above the basal level was found in the number of NSZs and F-actin content in osteoclasts transduced with FL-LPL (Fig. 3C, G, and H). A significant decrease below the basal level was observed in osteoclasts transduced with NT-LPL (Fig. 3D) or treated with a neutralizing antibody to TNF receptor 1 (TNFR-1; Fig. 3F). The number of NSZs and F-actin content are significantly reduced in these osteoclasts (panels G and H). Podosome like structures were also observed in osteoclasts transduced with NT-LPL or treated with a neutralizing antibody to TNF receptor 1 (Fig.3D and F; indicated by wavy arrows) It is also interesting to observe that the formation of podosome-like structures (indicated by wavy arrows) are not affected by NT-LPL peptide or neutralizing antibody to TNFR-1. However, impaired endogenous LPL phosphorylation abrogate the formation of NSZs and also the membrane extensions which assist in the spreading of osteoclasts.

Changes in NSZs formation in many osteoclasts transduced with various TAT-fused peptides are shown at lower magnification (Supplemental Figure 2). Transduction of HSV-TK or

mutated FL-LPL (A5A7) did not affect the formation of basal level NSZs (Figure S2; A and C). Failure of colocalization of these transduced peptides (green) with actin in these NSZs suggests that the endogenous or cellular LPL regulates the formation of these NSZs. Most remarkably, the colocalization (yellow) of the transduced FL-LPL peptide with actin (red) suggests that those NSZs are formed by the actin bundling process mediated by the transduced FL-LPL (B). Nevertheless, the number of NSZs are very minimal in osteoclasts transduced with NT-LPL (D). This observation establishes that NT-LPL peptide has the potential to efficiently suppress the actin bundling activity via competitive inhibition of endogenous LPL phosphorylation as shown in Fig. 2.

Analysis of the effect of transduced TAT fused LPL peptides on the formation of sealing rings and resorption pits in osteoclasts plated on dentine

Next, we proceeded to examine whether the inducible and inhibitory effects of FL-LPL and NT-LPL have an impact on the formation of fully functional sealing rings and bone resorption. Osteoclasts plated on dentine for 10–12h in the presence HSV-TK (Fig. 4A), FL-LPL (B), FL-LPL (A5A7; C), ABD (D), NT-LPL (E) and neutralizing antibody to TNFR-1 (F) were stained for actin with rhodamine phalloidin (red). Distribution of sealing rings (red color) and scans of dentine slices (green-pseudocolor) are shown (Figure 4). Sealing rings (indicated by the arrows in A-D) that are capable of resorbing the dentine matrix and pits were found underneath those sealing rings (overlay panels of A-C). Resorption pits were outlined with white lines in green panels representing dentine slice. Sealing rings counted in ~75 osteoclasts are provided in the graph (Fig. 4G). The number of sealing rings was increased in osteoclasts transduced with FL-LPL. Multiple sealing rings were observed in osteoclasts transduced with FL-LPL (Fig. 4; B and F) as compared with cells transduced with HSV-TK (A and F) or mutant FL-LPL (C). Multiple resorption pits underneath the sealing rings suggest that the sealing rings formed were efficient and functional. An increase in the number of sealing rings corresponds with an increase in the number and size (area) of resorption pits (Fig. 5; B and G). A significant decrease in the formation of NSZs (Fig. 3) with NT-LPL peptide corresponds with a reduction in sealing ring formation and resorption (Figs. 4 and 5; E and G). FL-LPL and NT-LPL have opposing effects on actin ring formation and resorption which indeed is comparable to their impact on the NSZs formation. A decrease in the number of NSZs and sealing rings (Figs. 3 and 4) by a neutralizing antibody to TNF receptor 1 (TNFR1) also corresponds with a decrease in resorption function (Fig. 5; F and G). These observations suggest that TNF-α signaling regulates LPL phosphorylation. NSZs seem to be the precursor zones from which maturation of fully functional sealing rings ensues.

Analysis of the effect of transduced TAT fused LPL peptides on the formation of podosomes and migration

LPL (aka fimbrin) was shown to localize in the podosomes of osteoclasts (14). However, studies on the role of LPL in actin modulation, podosome assembly/disassembly, and migration are limited. Having shown that NT-LPL peptide has the potential to reduce NSZs formation via suppressing the function of endogenous LPL in osteoclasts, we investigated whether this peptide would have a similar inhibitory effect on actin modulation involved in podosome assembly/disassembly and migration (Figure 6 A and B). TAT-fused FL-LPL (a),

mutated FLLPL (b), ABD (c), and NT-LPL (d) does not affect the actin modulation involved in podosome assembly/disassembly (Figure 6A) and migration (B). Actin staining was observed in the podosomes of osteoclast treated with indicated peptides. We conclude that LPL is indispensable to drive the actin bundling processes involved in sealing ring formation.

Together, these results support the role of LPL in the regulation of the formation of NSZs, a precursor zone for sealing rings by TNF-α signaling (schematic diagram in Figure 7).

Discussion

The process of sealing ring formation in osteoclasts requires significant actin filament reorganization; bundling and stability of actin filaments are fundamental steps in the formation of sealing rings, which allow osteoclasts to adhere to the bone surface tightly. Our results show that LPL regulates the actin bundling process at the early stage of sealing ring formation. Cooperativity between serine phosphorylation and actin binding to ABDs of LPL is required for the actin bundling process mediated by LPL. We have previously demonstrated a novel mechanistic link between LPL and cortactin in the formation of sealing ring. Cyclical changes in the levels of LPL protein and phosphorylation corresponded well with the actin cytoskeletal reorganization in resorbing osteoclasts. NSZs function as secondary adhesive sites during membrane extensions. Present results corroborate our previous observations [40] that polymerization of actin generates a force to push the plasma membrane forward to produce membrane extensions. NSZs formed at the extensions serve as adhesive structures which facilitate spreading of osteoclasts on bone.

It was understood that towards the beginning of the resorption phase, sealing rings are formed from the fusion of podosomes [31, 32, 58]. However, various findings have suggested that sealing rings formed on bone have a unique three-dimensional organization that is not derived from podosomes. Podosomes do not fuse together to form sealing rings on the dentine slice or mineralized matrix [29, 51]. It has also been suggested that podosomes may transform from individual dynamic structures to two-dimensional clusters. From these clusters, highly dynamic rings are formed, which eventually stabilize. This transition correlates with enhanced actin reorganization and a 10-fold increase in the amounts of F-actin [38]. Podosomes do not require adhering firmly to extracellular matrix (ECM) as they are rapidly constructed and removed. Their half-life is about 2–12min. [30]. The sealing ring is supposed to have very close and stable adhesion to ECM on the bone surface to generate tight sealing zone. Osteoclasts transduced with NT-LPL peptide did not have any effect on the actin modulation involved in the formation of podosomes. This suggests that the bundling of the actin filaments is not one of the processes involved in the formation of podosomes. However, NT-LPL peptide blocked the formation of NSZs. NSZs are several folds larger than the typical podosome structures. Our observations are consistent with the suggestions made by others [38] in the formation of actinrich aggregates before the establishment of sealing rings. Even so, if one considers that sealing rings are derived from podosomes, there should be remarkable changes in the reorganization of actin filaments because of the architectural nature of podosomes and sealing rings.

NSZs represent a part of the phenotypic changes that occur before the formation of sealing rings on mineralized matrix. L-Plastin is localized in NSZs and not in sealing rings of resorbing (Supplemental Figure 1); [40]. The contemporary view of actin reorganization in sealing ring formation and resorption activity have focused predominantly on integrin αvβ3 signaling [4, 24, 35, 41, 45, 50, 54, 57]. The limitation here is that the molecular mechanisms involved in the assembly of NSZs have not been studied. Osteoclasts from integrin β3 knockout mice [43] expressing a cytoplasmic domain deleted β3 constructs [18] or treated with echistatin, in fact have shown actin aggregates [18, 48]. It is possible that these aggregates may not be considered as an important zone at the time of these observations. Regulation of the formation of NSZs by TNF- α or RANKL signaling provides a new concept in osteoclast (OC) bone resorption (Scheme in Figure 7). Identification of formation of NSZs prior to sealing ring formation and localization of integrin αvβ3 in the NSZs provides a paradigm shift from the existing model of ″osteoclast adhesion to the bone surface➔assembly of sealing rings by αvβ3 signaling➔bone resorption" to the new model of ″osteoclast adhesion to the bone surface➔ formation of nascent sealing zones by TNF-α or RANKL signaling➔maturation of NSZs to sealing rings by αvβ3 signaling➔bone resorption″ (Figure 7).

Sealing rings consisting of bundled actin filaments that generate tight sealing zones on the bone surface. The areas encompassed by actin filaments in sealing rings range from 110μm [37]. Because of the architectural nature of sealing rings, a major reorganization of actin filaments is required during their formation. LPL was shown as one of the bundling proteins which cross-links actin filaments to tight bundles [19, 20, 36, 65]. Actin bundling is mediated by two tandem repeats of actin-binding domains (ABD) in LPL. These domains assist in binding two actin filaments into parallel arrays for bundle assembly [25, 49, 62]. Actin-binding proteins which have two discrete actin-binding domains nearby can achieve the process of actin bundling [65]. Although, osteoclasts express alpha (α)-actinin, which is also an actin-bundling protein, actin bundles generated by α-actinin are loose structures as seen in actin stress fibers [37, 42]. ABDs are placed at a distance in α-actinin and separated by a helical spacer region which may cause the formation of a different actin bundling feature. LPL seems to be an appropriate protein in the tight bundling of actin filaments essential for osteoclast bone resorption. LPL was also shown to stabilize actin filaments and protect them against depolymerization [34], which is a must for the efficient function of the sealing ring during bone resorption. Osteoclasts treated with Enoxacin demonstrated proteolytic processing of several proteins. LPL was identified as one of the cytoskeletal proteins. Treatment with enoxacin reduced the association of V-ATPase subunits with the detergent-insoluble cytoskeleton. It is possible that the amount of insoluble cytoskeleton may be reduced in these osteoclasts due to failure in the formation of actin aggregates by the cleavage of LPL [60].

Phosphorylation of LPL on Ser-5 and −7 residues was shown to be essential for actin binding/bundling activity of LPL [26]. In this paper, transduction of TAT-fused NT-LPL peptide into osteoclasts allowed us to correlate the observed actin modulation with LPL functional domains. Analyses with TAT-fused LPL peptides not only revealed the feasibility of the techniques but also the ability of the peptides to induce changes in the actin cytoskeleton of resorbing osteoclasts. An increase in F-actin content, number of NSZs and

sealing rings in osteoclasts transduced with FL-LPL peptide showed the significance of LPL in the formation of NSZs. L-plastin was suggested to affect actin turn-over via decreasing the actin dissociation rate by several-fold, thereby increasing the amount of F-actin [1]. As suggested by others [1], it is possible that the transduced FL-LPL may have a similar effect on decreasing the actin turn over which reflects on the amount of F-actin and the number of NSZs. L-plastin binding with Factin may assist in the assembly and bundling of actin filaments. Bundling of actin filaments is crucial in the formation/function of the sealing ring as opposed to podosomes which are highly turn-over structures. High turnover of actin filament in fact is necessary for podosome assembly/disassembly because osteoclasts are highly motile cells [9]. LPL was shown to present in the podosomes of macrophages. It promotes the longevity and provides support to the migration of macrophages. Podosome stability is disrupted in primary resident peritoneal macrophages from $LPL^{-/-}$ mice [66]. Competitive inhibition of serine phosphorylation of cellular LPL by NT-LPL peptide reduced the formation of NSZs. It did not affect the assembly of podosomes or migration. Further analyses in osteoclasts isolated from $LPL^{-/-}$ mice will substantiate the role of LPL in actin dynamics involved in osteoclast sealing ring formation and bone resorption.

NT-LPL peptide exerts inhibitory effects on the function of cellular LPL as assayed by the levels of phosphorylation of cellular LPL, changes in actin dynamics, and capacity to resorb bone. Non-phosphorylated LPL was shown to have lesser interaction with the actin cytoskeleton in Vero cells [1]. Serine phosphorylation not only increases the affinity of LPL with actin filaments but also the localization of integrin in nascent sealing zones which is required for the maturation of NSZs to sealing rings and bone resorption. We show here that the transduction of mutated FL- LPL (A5A7) had no additional effect on the actin bundling process and NSZ formation although it contains other domains such as ABDs and EF-hand. This suggests that serine phosphorylation of LPL modulates the actin bundling processes involved in the formation of NSZs. Understanding the regulation of serine phosphorylation is vital in the evaluation of the role of LPL in osteoclast function. Cooperativity between serine phosphorylation and actin binding to ABDs is required for the actin bundling process mediated by LPL. Hence, the transduction of ABD alone did not affect the function of cellular LPL. The data derived from experiments with NT-LPL, ABD and mutated FL-LPL at serine residues elucidate the specific role of LPL phosphorylation on NSZs formation. Serine phosphorylation of LPL is a necessary process in the effects mediated by ABD such as bundling and stabilization of actin filaments. Therefore, no additional effects in the formation of actin aggregates were observed in osteoclasts transduced with either mutated FL-LPL (A5A7) or ABD.

LPL was shown to make a complex with cortactin [1] and integrin beta (β1 & β3) subunits [33] and regulates actin dynamics in carcinoma cells. Cortactin associates with integrins [55, 56, 63], and also found in the sealing rings of osteoclasts in a time-dependent manner [12, 40]. Although ABDs of LPL has no phosphorylation sites, it can bind to the cytoplasmic domain of integrin β-subunit and make a complex with cortactin [33]. We have previously shown the localization of cortactin in nascent sealing zones besides integrin αv or β3. This complex regulates the maturation of sealing zones to rings in osteoclasts [11, 12, 40]. LPL was not observed in nascent sealing zones at the time of maturation, i.e. from 6h onwards; although the diffuse cellular distribution of LPL was observed [40]. Moreover, the

interaction of integrin with F-actin was maximal from 6h onwards. Therefore, we suggest that ABD/ F-actin interaction is cell-type specific, and LPL may not be a direct integrin scaffold for F-actin binding in osteoclasts. Further detail studies are required to determine how ABDs function in the bundling of actin filaments.

Conclusions:

The findings herein, a) indicate that phosphorylation of LPL on serine residues regulate actin bundling via two ABDs. b) demonstrate the significance of LPL phosphorylation and function in NSZs formation at the early stage of sealing ring formation. c) demonstrate that phosphorylation of LPL acts as an integrator of signals that control the actin bundling action. d) show that LPL stabilizes actin bundles to mature into sealing rings. To our knowledge, this is the first study to cast light on the role of LPL phosphorylation on actin bundling process involved in the formation of NSZs in osteoclasts subjected to bone resorption. These studies identify LPL as a novel therapeutic target in osteoclast-mediated events.

Supplementary Material

Refer to Web version on PubMed Central for supplementary material.

Acknowledgments

Research reported in this publication was supported by the National Institute of Arthritis and Musculoskeletal and Skin Diseases of the National Institutes of Health under Award Number R01 AR066044 to M.C. The content is solely the responsibility of the authors and does not necessarily represent the official views of the National Institutes of Health. Authors gratefully acknowledge Dr. Steven Dowdy (Professor of Cellular and Molecular Medicine; University of California San Diego; School of Medicine) for the pTAT-HA vector and pTAT-HSV-TK construct.

Abbreviations

Gsn−/−	gelsolin null
ABP	actin-binding protein
RANKL	receptor activator of NF-κB ligand
MCSF	macrophage colony stimulating factor
LPL	L-Plastin
TAT	transactivator peptide with transforming properties
FL-LPL	full-length L-plastin
NT-LPL	amino-terminal L-plastin peptide
ABD	actin-binding domain
TNF-α	tumor necrosis factor alpha
TAT	transactivator peptide with transforming properties

NSZ	nascent sealing zone
integrin αvβ3	cell surface receptor aka vitonectin receptor
F-actin	filamentous actin
ECM	extracellular matrix

Reference List

[1]. Al TZ, Schaffner-Reckinger E, Halavatyi A, Hoffmann C, Moes M, Hadzic E, Catillon M, Yatskou M, Friederich E, Quantitative kinetic study of the actin-bundling protein L-plastin and of its impact on actin turn-over. PLoS.ONE. 5 (2010) e9210. [PubMed: 20169155]

[2]. Arpin M, Friederich E, Algrain M, Vernel F, Louvard D, Functional differences between L- and T-plastin isoforms. J.Cell Biol 127 (1994) 1995–2008. [PubMed: 7806577]

[3]. Babb SG, Matsudaira P, Sato M, Correia I, Lim S-S, Fimbrin in podosomes of monocyte-derived osteoclasts. Cell Motil.Cytosk. 37 (1997) 308–325.

[4]. Batsir S, Geiger B, Kam Z, Dynamics of the sealing zone in cultured osteoclasts. Cytoskeleton (Hoboken.) 74 (2017) 72–81. [PubMed: 27997747]

[5]. Biswas R, Yuen D, Hruska K, MA. Chellaiah. Functional assessment of specific gelsolin peptide domains in osteoclast Actin Assembly and Motility. J Bone Miner Res 18 suppl1[Functional assessment of specific gelsolin peptide domains in osteoclast Actin Assembly and Motility], S279 10-10-2003.

[6]. Bretscher A, Purification of the intestinal microvillus cytoskeletal proteins villin, fimbrin, and ezrin. Methods Enzymol. 134 (1986) 24–37. [PubMed: 3821564]

[7]. Chellaiah M, Fitzgerald C, Alvarez U, Hruska K, C-*src* is required for stimulation of gelsolin associated PI3-K. J.Biol.Chem 273 (1998) 11908–11916. [PubMed: 9565618]

[8]. Chellaiah M, Hruska KA, Osteopontin stimulates gelsolin associated phosphoinositide levels and PtdIns 3-hydroxyl kinase. Mol.Biol.Cell 7 (1996) 743–753. [PubMed: 8744948]

[9]. Chellaiah M, Kizer N, Silva M, Alvarez U, Kwiatkowski D, Hruska KA, Gelsolin deficiency blocks podosome assembly and produces increased bone mass and strength. J.Cell Biol 148 (2000) 665–678. [PubMed: 10684249]

[10]. Chellaiah M, Soga N, Swanson S, McAllister S, Alvarez U, Wang D, Dowdy SF, Hruska KA, Rho-A is critical for osteoclast podosome organization, motility, and bone resorption. J.Biol.Chem 275 (2000) 11993–12002. [PubMed: 10766830]

[11]. Chellaiah MA, Kuppuswamy D, Lasky L, Linder S, Phosphorylation of a WiscottAldrich syndrome protein-associated signal complex is critical in osteoclast bone resorption. J.Biol.Chem 282 (2007) 10104–10116. [PubMed: 17283076]

[12]. Chellaiah MA, Schaller MD, Activation of Src kinase by protein-tyrosine phosphatasePEST in osteoclasts: comparative analysis of the effects of bisphosphonate and proteintyrosine phosphatase inhibitor on Src activation in vitro. J.Cell Physiol 220 (2009) 382393.

[13]. Chen H, Mocsai A, Zhang H, Ding RX, Morisaki JH, White M, Rothfork JM, Heiser P, Colucci-Guyon E, Lowell CA, Gresham HD, Allen PM, Brown EJ, Role for plastin in host defense distinguishes integrin signaling from cell adhesion and spreading. Immunity. 19 (2003) 95–104. [PubMed: 12871642]

[14]. de Arruda MV, Watson S, Lin CS, Leavitt J, Matsudaira P, Fimbrin is a homologue of the cytoplasmic phosphoprotein plastin and has domains homologous with calmodulin and actin gelation proteins. J.Cell Biol 111 (1990) 1069–1079. [PubMed: 2391360]

[15]. Delanote V, Vandekerckhove J, Gettemans J, Plastins: versatile modulators of actin organization in (patho)physiological cellular processes. Acta Pharmacol.Sin 26 (2005) 769–779. [PubMed: 15960882]

[16]. Desai B, Ma T, Chellaiah MA, Invadopodia and matrix degradation: a new property of prostate cancer cells during migration and invasion. J.Biol.Chem.2008).

[17]. Desai B, Ma T, Zhu J, Chellaiah MA, Characterization of the expression of variant and standard CD44 in prostate cancer cells: identification of the possible molecular mechanism of CD44/MMP9 complex formation on the cell surface. J.Cell Biochem 108 (2009) 272–284. [PubMed: 19582779]

[18]. Feng X, Novack DV, Faccio R, Ory DS, Aya K, Boyer MI, McHugh KP, Ross FP, Teitelbaum SL, A Glanzmann's mutation in beta 3 integrin specifically impairs osteoclast function. J Clin.Invest 107 (2001) 1137–1144. [PubMed: 11342577]

[19]. Foran E, McWilliam P, Kelleher D, Croke DT, Long A, The leukocyte protein L-plastin induces proliferation, invasion and loss of E-cadherin expression in colon cancer cells. Int.J.Cancer 118 (2006) 2098–2104. [PubMed: 16287074]

[20]. Frederick MJ, Rodriguez LV, Johnston DA, Darnay BG, Grimm EA, Characterization of the M(r) 65,000 lymphokine-activated killer proteins phosphorylated after tumor target binding: evidence that pp65a and pp65b are phosphorylated forms of L-plastin. Cancer Res. 56 (1996) 138–144. [PubMed: 8548753]

[21]. Freeley M, O'Dowd F, Paul T, Kashanin D, Davies A, Kelleher D, Long A, L-plastin regulates polarization and migration in chemokine-stimulated human T lymphocytes. J.Immunol 188 (2012) 6357–6370. [PubMed: 22581862]

[22]. Fuller K, Kirstein B, Chambers TJ, Murine osteoclast formation and function: differential regulation by humoral agents. Endocrinology 147 (2006) 1979–1985. [PubMed: 16384864]

[23]. Fuller K, Murphy C, Kirstein B, Fox SW, Chambers TJ, TNFalpha potently activates osteoclasts, through a direct action independent of and strongly synergistic with RANKL. Endocrinology 143 (2002) 1108–1118. [PubMed: 11861538]

[24]. Georgess D, Machuca-Gayet I, Blangy A, Jurdic P, Podosome organization drives osteoclast-mediated bone resorption. Cell Adh.Migr 8 (2014) 191–204. [PubMed: 24714644]

[25]. Hanein D, Volkmann N, Goldsmith S, Michon AM, Lehman W, Craig R, DeRosier D, Almo S, Matsudaira P, An atomic model of fimbrin binding to F-actin and its implications for filament crosslinking and regulation. Nat.Struct.Biol 5 (1998) 787–792. [PubMed: 9731773]

[26]. Janji B, Giganti A, De C, Catillon VM, Bruyneel E, Lentz D, Plastino J, Gettemans J, Friederich E, Phosphorylation on Ser5 increases the F-actin-binding activity of L-plastin and promotes its targeting to sites of actin assembly in cells. J.Cell Sci 119 (2006) 1947–1960. [PubMed: 16636079]

[27]. Jones SL, Brown EJ, FcgammaRII-mediated adhesion and phagocytosis induce Lplastin phosphorylation in human neutrophils. J.Biol.Chem 271 (1996) 14623–14630. [PubMed: 8663066]

[28]. Jones SL, Wang J, Turck CW, Brown EJ, A role for the actin-bundling protein Lplastin in the regulation of leukocyte integrin function. Proc.Natl.Acad.Sci.U.S.A 95 (1998) 9331–9336. [PubMed: 9689080]

[29]. Jurdic P, Saltel F, Chabadel A, Destaing O, Podosome and sealing zone: specificity of the osteoclast model. Eur.J.Cell Biol 85 (2006) 195–202. [PubMed: 16546562]

[30]. Kanehisa J, Yamanaka T, Doi S, Turksen K, Heersche JNM, Aubin JE, Takeuchi H, A band of F-actin containing podosomes is involved in bone resorption by osteoclasts. Bone 11 (1990) 287–293. [PubMed: 2242294]

[31]. Lakkakorpi PT, Vaananen HK, Kinetics of the osteoclast cytoskeleton during the resorption cycle *in vitro*. J.Bone Miner.Res 6 (1991) 817–826. [PubMed: 1664645]

[32]. Lakkakorpi PT, Vaananen HK, Cytoskeletal changes in osteoclasts during the resorption cycle. Microsc Res Tech 33 (1996) 171–181. [PubMed: 8845516]

[33]. Le GE, Vallentin A, Harmand PO, drian-Herrada G, Rebiere B, Roy C, Benyamin Y, Lebart MC, Characterization of L-plastin interaction with beta integrin and its regulation by micro-calpain. Cytoskeleton (Hoboken.) 67 (2010) 286–296. [PubMed: 20183869]

[34]. Lebart MC, Hubert F, Boiteau C, Venteo S, Roustan C, Benyamin Y, Biochemical characterization of the L-plastin-actin interaction shows a resemblance with that of alpha-actinin and allows a distinction to be made between the two actin-binding domains of the molecule. Biochemistry 43 (2004) 2428–2437. [PubMed: 14992580]

[35]. Lee EJ, Kim JL, Gong JH, Park SH, Kang YH, Inhibition of osteoclast activation by phloretin through disturbing alphavbeta3 integrin-c-Src pathway. Biomed.Res.Int 2015 (2015) 680145. [PubMed: 25834823]

[36]. Lin CS, Lau A, Yeh CC, Chang CH, Lue TF, Upregulation of L-plastin gene by testosterone in breast and prostate cancer cells: identification of three cooperative androgen receptor-binding sequences. DNA Cell Biol. 19 (2000) 1–7. [PubMed: 10668786]

[37]. Luxenburg C, Addadi L, Geiger B, The molecular dynamics of osteoclast adhesions. Eur.J.Cell Biol 85 (2006) 203–211. [PubMed: 16360241]

[38]. Luxenburg C, Geblinger D, Klein E, Anderson K, Hanein D, Geiger B, Addadi L, The architecture of the adhesive apparatus of cultured osteoclasts: from podosome formation to sealing zone assembly. PLoS.ONE. 2 (2007) e179. [PubMed: 17264882]

[39]. Ma T, Chellaiah MA. Disruption of WASP associated signaling complex formation leads to defects in sealing ring formation and bone resorption in osteoclasts. J Bone and Min Research 2007. 2007.

[40]. Ma T, Sadashivaiah K, Chellaiah MA, Regulation of sealing ring formation by L-plastin and cortactin in osteoclasts. J.Biol.Chem 285 (2010) 29911–29924. [PubMed: 20650888]

[41]. Ma T, Samanna V, Chellaiah MA, Dramatic inhibition of osteoclast sealing ring formation and bone resorption in vitro by a WASP-peptide containing pTyr294 amino acid. J.Mol.Signal. 3 (2008) 4. [PubMed: 18289379]

[42]. Marchisio PC, Cirillo D, Teti A, Zambonin-Zallone A, Tarone G, Rous sarcoma virustransformed fibroblasts and cells of monocytic origin display a peculiar dot-like organization of cytoskeletal proteins involved in microfilament-membrane interactions. Exp.Cell Res 169 (1987) 202–214. [PubMed: 3028844]

[43]. McHugh KP, Hodivala-Dilke K, Zheng M-H, Namba N, Lam J, Novack D, Feng X, Ross FP, Hynes RO, Teitelbaum SL, Mice lacking β3 integrins are osteosclerotic because of dysfunctional osteoclasts. J.Clin.Invest 105 (2000) 433–440. [PubMed: 10683372]

[44]. Messier JM, Shaw LM, Chafel M, Matsudaira P, Mercurio AM, Fimbrin localized to an insoluble cytoskeletal fraction is constitutively phosphorylated on its headpiece domain in adherent macrophages. Cell Motil.Cytoskeleton 25 (1993) 223–233. [PubMed: 8221900]

[45]. Miyazaki T, Sanjay A, Neff L, Tanaka S, Horne WC, Baron R, Src kinase activity is essential for osteoclast function. J.Biol.Chem 279 (2004) 17660–17666. [PubMed: 14739300]

[46]. Morley SC, The actin-bundling protein L-plastin: a critical regulator of immune cell function. Int.J.Cell Biol 2012 (2012) 935173. [PubMed: 22194750]

[47]. Nagahara H, Vocero-Akbani AM, Snyder EL, Ho A, Latham DG, Lissy NA, Becker-Hapak M, Ezhevsky SA, Dowdy SF, Transduction of full-length TAT fusion proteins into mammalian cells: TAT-$p27^{Kip1}$ induces cell migration. Nature Medicine 4 (1998) 1449–1452.

[48]. Nakamura I, Pilkington MF, Lakkakorpi PT, Lipfert L, Sims SM, Dixon SJ, Rodan GA, Duong LT, Role of alpha(v)beta(3) integrin in osteoclast migration and formation of the sealing zone. J.Cell Sci 112 (Pt 22) (1999) 3985–3993. [PubMed: 10547359]

[49]. Namba Y, Ito M, Zu Y, Shigesada K, Maruyama K, Human T cell L-plastin bundles actin filaments in a calcium-dependent manner. J.Biochem.(Tokyo) 112 (1992) 503–507. [PubMed: 1491005]

[50]. Novack DV, Faccio R, Osteoclast motility: putting the brakes on bone resorption. Ageing Res.Rev 10 (2011) 54–61. [PubMed: 19788940]

[51]. Saltel F, Destaing O, Bard F, Eichert D, Jurdic P, Apatite-mediated Actin Dynamics in Resorbing Osteoclasts. Mol.Biol.Cell 2004).

[52]. Schneider C, Sepp-Lorenzino L, Nimmesgern E, Ouerfelli O, Danishefsky S, Rosen N, Hartl FU, Pharmacologic shifting of a balance between protein refolding and degradation mediated by Hsp90. Proc.Natl.Acad.Sci.U.S.A 93 (1996) 14536–14541. [PubMed: 8962087]

[53]. Shibata M, Ohoka T, Mizuno S, Suzuki K, Characterization of a 64-kd protein phosphorylated during chemotactic activation with IL-8 and fMLP of human polymorphonuclear leukocytes. I. Phosphorylation of a 64-kd protein and other proteins. J.Leukoc.Biol 54 (1993) 1–9. [PubMed: 8393062]

[54]. Soysa NS, Alles N, Osteoclast function and bone-resorbing activity: An overview. Biochem.Biophys.Res.Commun 476 (2016) 115–120. [PubMed: 27157135]

[55]. Spinardi L, Marchisio PC, Podosomes as smart regulators of cellular adhesion. Eur.J Cell Biol 85 (2006) 191–194. [PubMed: 16546561]

[56]. Spinardi L, Rietdorf J, Nitsch L, Bono M, Tacchetti C, Way M, Marchisio PC, A dynamic podosome-like structure of epithelial cells. Exp.Cell Res 295 (2004) 360–374. [PubMed: 15093736]

[57]. Teitelbaum SL, The osteoclast and its unique cytoskeleton. Ann.N.Y.Acad.Sci 1240 (2011) 14–17. [PubMed: 22172034]

[58]. Teti A, Marchisio PC, Zambonin-Zallone A, Clear zone in osteoclast function: role of podosomes in regulation of bone-resorbing activity (Review). Amer.J.Physiol 261 (1991) C1–C7. [PubMed: 1858848]

[59]. Todd EM, Deady LE, Morley SC, The actin-bundling protein L-plastin is essential for marginal zone B cell development. J.Immunol 187 (2011) 3015–3025. [PubMed: 21832165]

[60]. Toro EJ, Ostrov DA, Wronski TJ, Holliday LS, Rational identification of enoxacin as a novel V-ATPase-directed osteoclast inhibitor. Curr.Protein Pept.Sci 13 (2012) 180191.

[61]. Vocero-Akbani A, Chellaiah MA, Hruska KA, Dowdy SF, Protein transduction: delivery of Tat-GTPase fusion proteins into mammalian cells. Meth.Enzymol 332, 36–49. 2001. [PubMed: 11305111]

[62]. Volkmann N, DeRosier D, Matsudaira P, Hanein D, An atomic model of actin filaments cross-linked by fimbrin and its implications for bundle assembly and function. J.Cell Biol 153 (2001) 947–956. [PubMed: 11381081]

[63]. Vuori K, Ruoslahti E, Tyrosine phosphorylation of p130Cas and cortactin accompanies integrin-mediated cell adhesion to extracellular matrix. J Biol.Chem 270 (1995) 2225922262.

[64]. Wang C, Morley SC, Donermeyer D, Peng I, Lee WP, Devoss J, Danilenko DM, Lin Z, Zhang J, Zhou J, Allen PM, Brown EJ, Actin-bundling protein L-plastin regulates T cell activation. J Immunol. 185 (2010) 7487–7497. [PubMed: 21076065]

[65]. Winder SJ, Ayscough KR, Actin-binding proteins. J.Cell Sci. 118 (2005) 651–654. [PubMed: 15701920]

[66]. Zhou JY, Szasz TP, Stewart-Hutchinson PJ, Sivapalan J, Todd EM, Deady LE, Cooper JA, Onken MD, Morley SC, L-Plastin promotes podosome longevity and supports macrophage motility. Mol.Immunol 78 (2016) 79–88. [PubMed: 27614263]

Highlights:

- Phosphorylation of L-plastin (LPL) by TNF-α signaling regulates actin bundling process involved in the formation of nascent sealing zones
- Nascent sealing zones are considered as precursor zones for the matured sealing rings
- This is the first study to cast light on the role of LPL phosphorylation on actin bundling process involved in the formation of NSZs in osteoclasts subjected to bone resorption
- Studies in this paper identify LPL as a possible novel therapeutic target in osteoclast-mediated events.

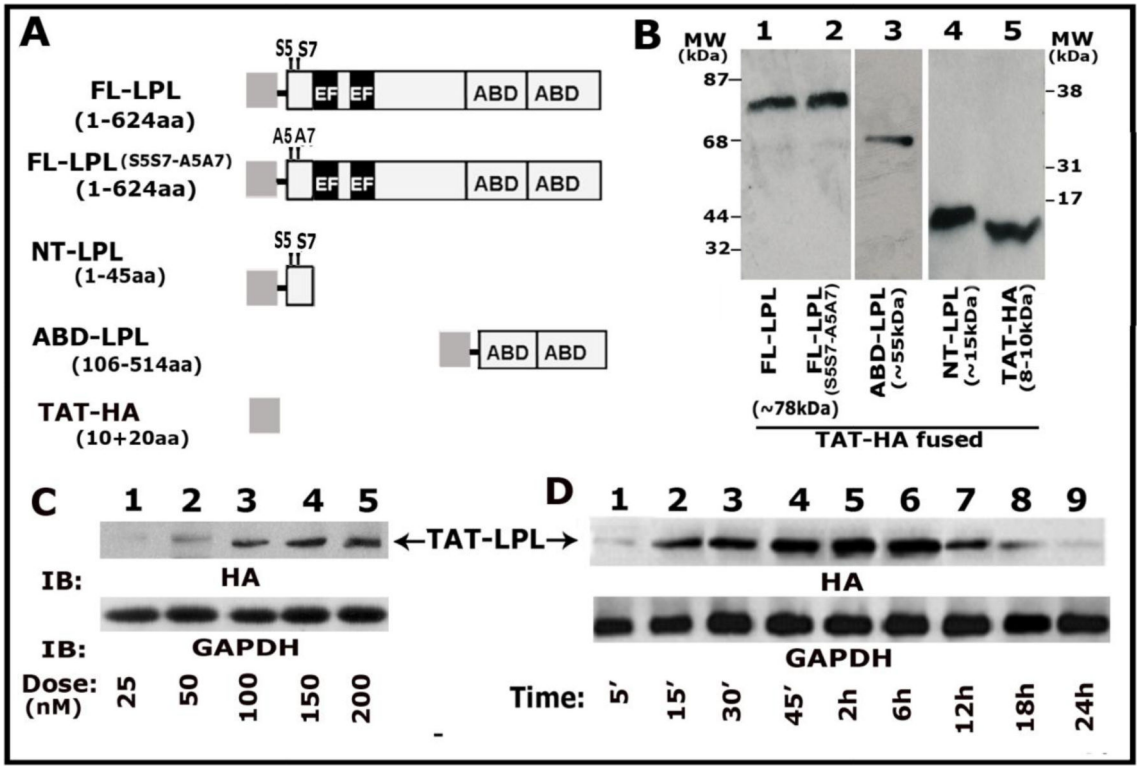

Figure 1: Purification and analysis of dose and time-dependent uptake of TAT-fused LPL peptides.

Schematic diagram demonstrating various LPL constructs generated in a pTAT-HA expression vector is shown (Panel A). The domain organization of LPL is shown in full-length LPL (FL-LPL). The following are cloned separately into the pTAT-HA expression vector: FL-LPL, mutated FLLPL (A5A7), amino-terminal LPL containing S5 and S7 (NT-LPL), and actin-binding domains of LPL (ABD-LPL). The number within the parentheses indicates the first and last amino acid of the corresponding LPL peptide. The expression vector contains TAT protein transduction domain (10aa) and an HA- tag (20aa). *S*DS-PAGE analysis of purified TAT-fused LPL peptides is shown in Panel B. TAT-fused peptides were subjected to 8% (lanes 1 −3) and 15% (lanes 4 and 5) SDS-PAGE and stained with Coomassie blue. The purified proteins and their approximate molecular mass (kDa) are indicated below each lane. The standard molecular weight markers (kDa) are also indicated for 8% (left) and 15% (right) polyacrylamide gels (Panel B). Demonstration of a dose- and time-dependent uptake of TAT-fused FL-LPL in osteoclasts (Panels C and D). Immunoblotting analysis with an HA antibody was done to detect the transduced protein levels in osteoclast lysates. The blot was stripped and blotted with a GAPDH antibody for normalization (bottom panels of C and D). The results shown in B-D are representative of two different experiments from two different osteoclasts and TAT-protein preparations.

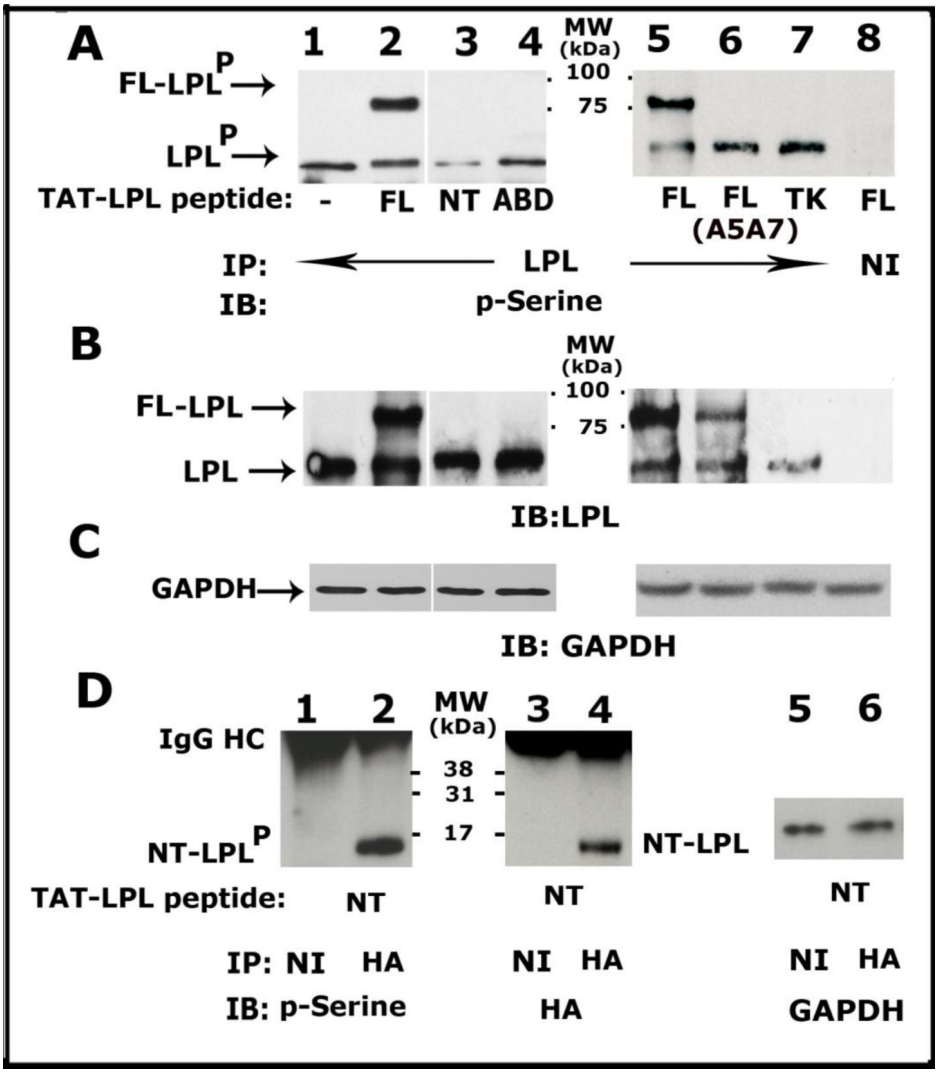

Figure 2: Immunoblotting analysis of phosphorylation of transduced and endogenous LPL protein in lysates made from osteoclasts

Osteoclasts treated with bone particles and TNF-α were also transduced with the following TATfused LPL and control (HSV-TK) peptides (150nM) for 3h as described in the Methods section: FL-LPL (Panel A; lanes 2 and 5); mutated FL-LPL (A5A7; lane 6); NT-LPL (lane 3), ABD-LPL (lane 4), and HSV-TK (lane 7). Lysates were immunoprecipitated with an antibody to LPL (lanes 1–7), HA (Panel D) or non-immune serum (NI; Panels A and D). The immunoprecipitates were subjected to 10% (Panel A) or 15% (Panel D) SDS-PAGE and immunoblotted with an antibody to phosphoserine (p-Serine; Panels A and D-lanes 1 and 2). Phosphorylated transduced LPL peptides and endogenous LPL protein are indicated in panels A and B. Stripping and reblotting of blot A with an antibody to LPL showed endogenous LPL and transduced FL-LPL (Panel B). Stripping and reblotting of blot D (left) with an antibody to HA shows the immunoprecipitated levels of transduced NT-LPL peptides (lane 4). Equal amount of total protein (Input) used for immunoprecipitation was assessed by direct immunoblotting of the lysates with a GAPDH antibody (Panels C and D-

lanes 5 and 6). The results shown are representative of three different experiments from three different osteoclast preparations.

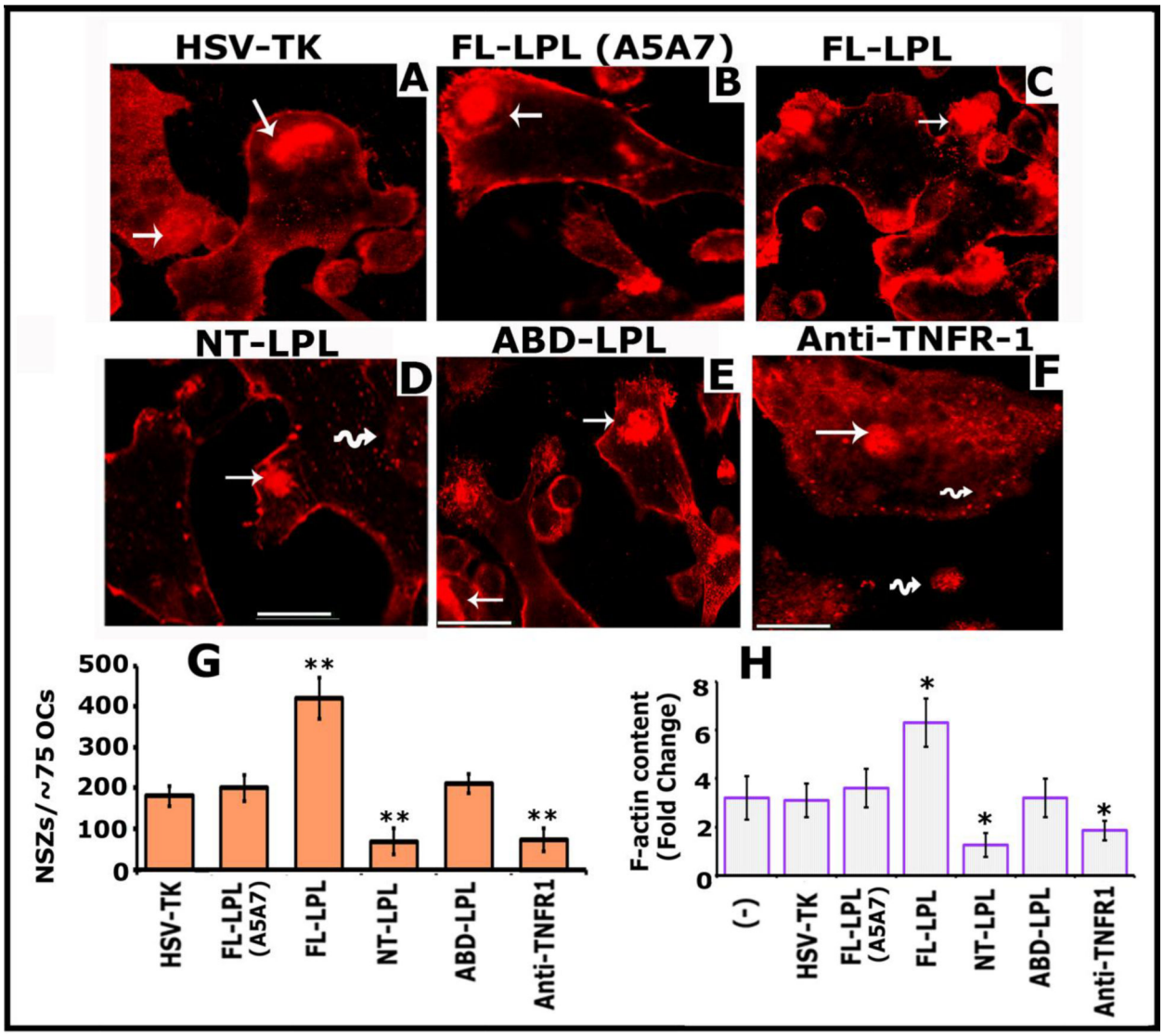

Figure 3: The effect of transduction of indicated TAT- LPL peptides on the formation of NSZs and total cellular F-actin content

Osteoclasts transduced with indicated LPL peptides were plated on dentine slices and incubated for 3–4h with TNF-α. Staining was performed with rhodamine-phalloidin for actin. Confocal images of osteoclasts are shown (Panels A-F). Arrows point to NSZs. Wavy arrows point to podosome-like structures. Scale bar-25μm. The number of NSZs were counted in ~ 75 osteoclasts and provided as a graph (Panel G). The data shown are the mean ± SEM of one of the three experiments performed with the same results. **p<0.01 versus HSV-TK transduced cells. F-actin content levels were determined by rhodamine-phalloidin binding to osteoclasts treated with anti-TNFR1 antibody as well as transduced or untransduced with indicated TATLPL peptides (Panel H). The F-actin content of the 0-min cells was assigned a value of 1.0 and all other values were expressed relative to the 0-mins values Values plotted are mean ± SD from three experiments *p<0.05 versus untreated (−) or HSV-TK transduced cells.

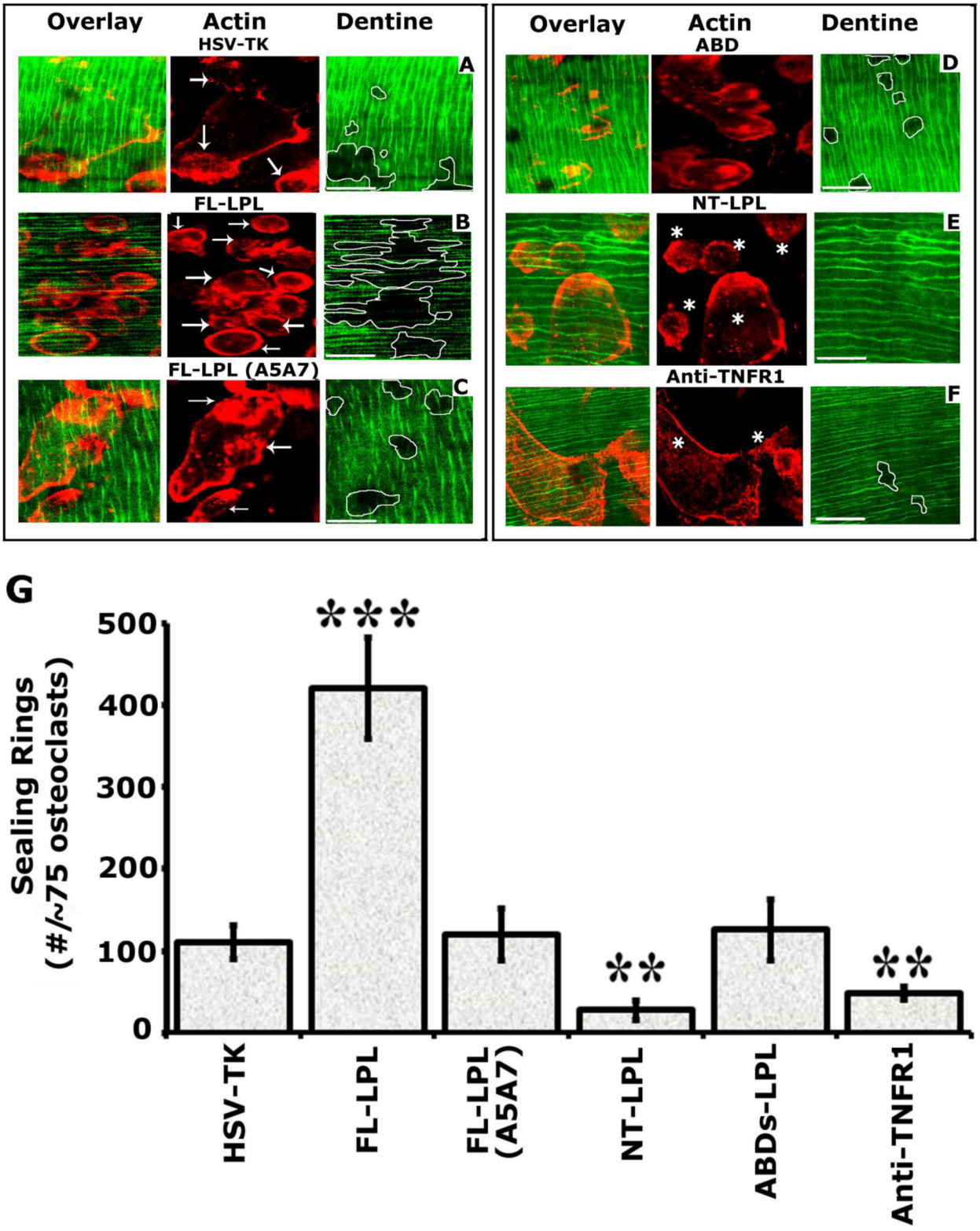

Figure 4: Analysis of the formation of sealing rings and resorption in osteoclasts

Osteoclasts transduced with indicated TAT-fused HSV-TK (A) and LPL (B-D) peptides were plated on dentine slices and incubated for 10–12h with TNF-α. Some cultures were treated

with a neutralizing antibody to TNFR-1 (E). Confocal microscopy images of osteoclasts stained for actin (red) is shown. The reflected light in green is dentine. Overlay images show the distribution of actin protein (red) in osteoclasts plated on dentine slices (green). Resorption pits were found underneath where sealing rings were found in osteoclasts (indicated by arrows in red panels; AC). Resorption pits were outlined with white lines in green panels (A-C). Asterisks indicate punctate podosome-like structures in osteoclasts transduced with NT-LPL (panel D) or treated with a neutralizing antibody to TNFR-1 (E). Scale bar- 25μm. These results represent one of the three experiments performed with the similar results.. Sealing rings were counted in ~75 osteoclasts and provided as a graph in panel G; mean ±SEM. *** $p<0.001$; **$p<0.01$ versus HSV-TK transduced cells. Data provided are the representative of at least three independent experiments with comparable results.

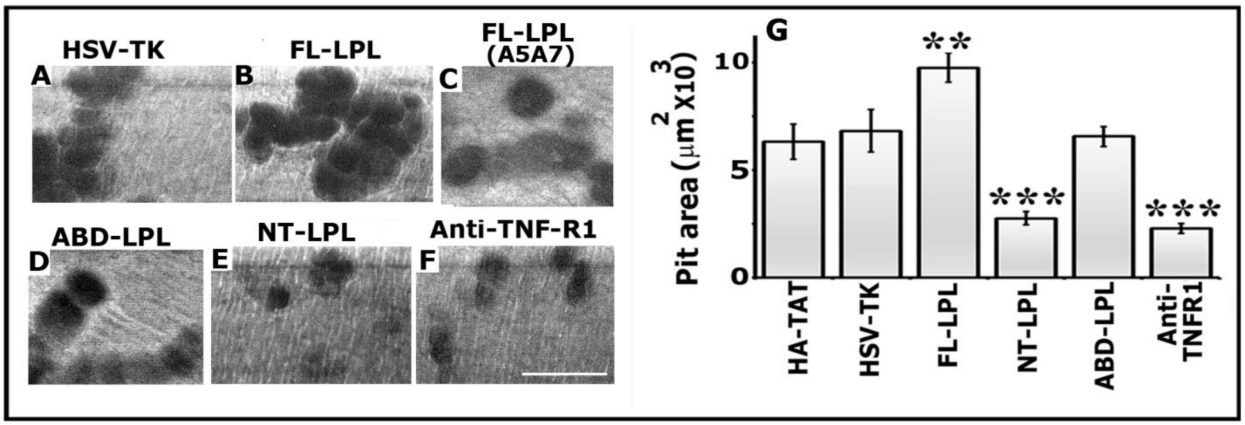

Figure 5:

Analysis of the effects of transduced TAT-LPL peptides on resorption by osteoclasts using dentine slices. Osteoclasts transduced with indicated TAT-fused peptides (Panels A-E) or treated with a neutralizing antibody to TNFR-1 (panel F) were cultured on dentine slices for 1012 h in the presence of TNF-α. Pits were scanned in a Bio-Rad confocal microscopy. Scale bar- 25μm. Resorbed area is seen as dark areas. Statistic measurements for the pit area are provided as a graph in G. ***$p<0.001$ and **$p<0.05$ versus HSV-TK transduced cells. The resorbed pit areas (20–25 pits/slice) were quantified and data were compiled from four slices per treatment. The data showed (G) is the mean±SEM of one experiment performed. Experiments were repeated three times with three different osteoclast preparations.

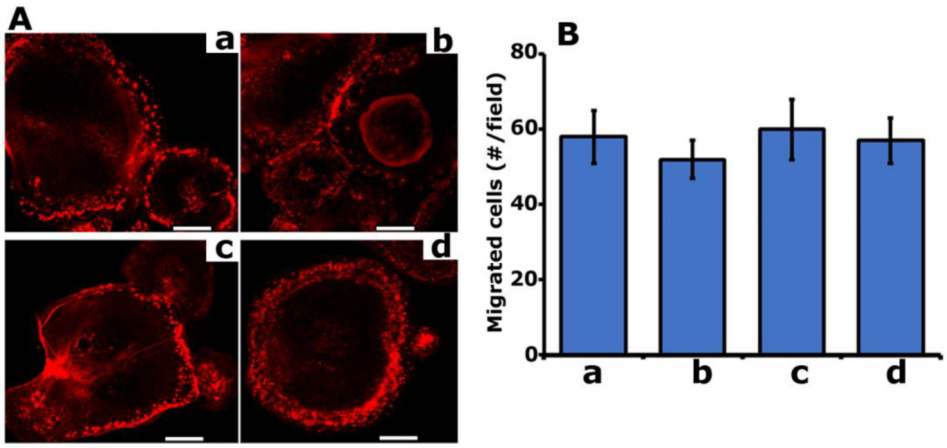

Figure 6:

Analysis of the effect of TAT-fused LPL peptides on actin distribution in podosomes and migration. A. Actin staining with rhodamine phalloidin. TAT-fused FL-LPL (a), mutated FLLPL (b), ABD (c), and NT-LPL (d) were used. Confocal microscopy analysis of the actin stained cells is shown. Scale bar-25μm. B. Transwell migration assay. Data are presented as the number of cells per migrated field (mean ± SD) from one experiment of the three experiments performed

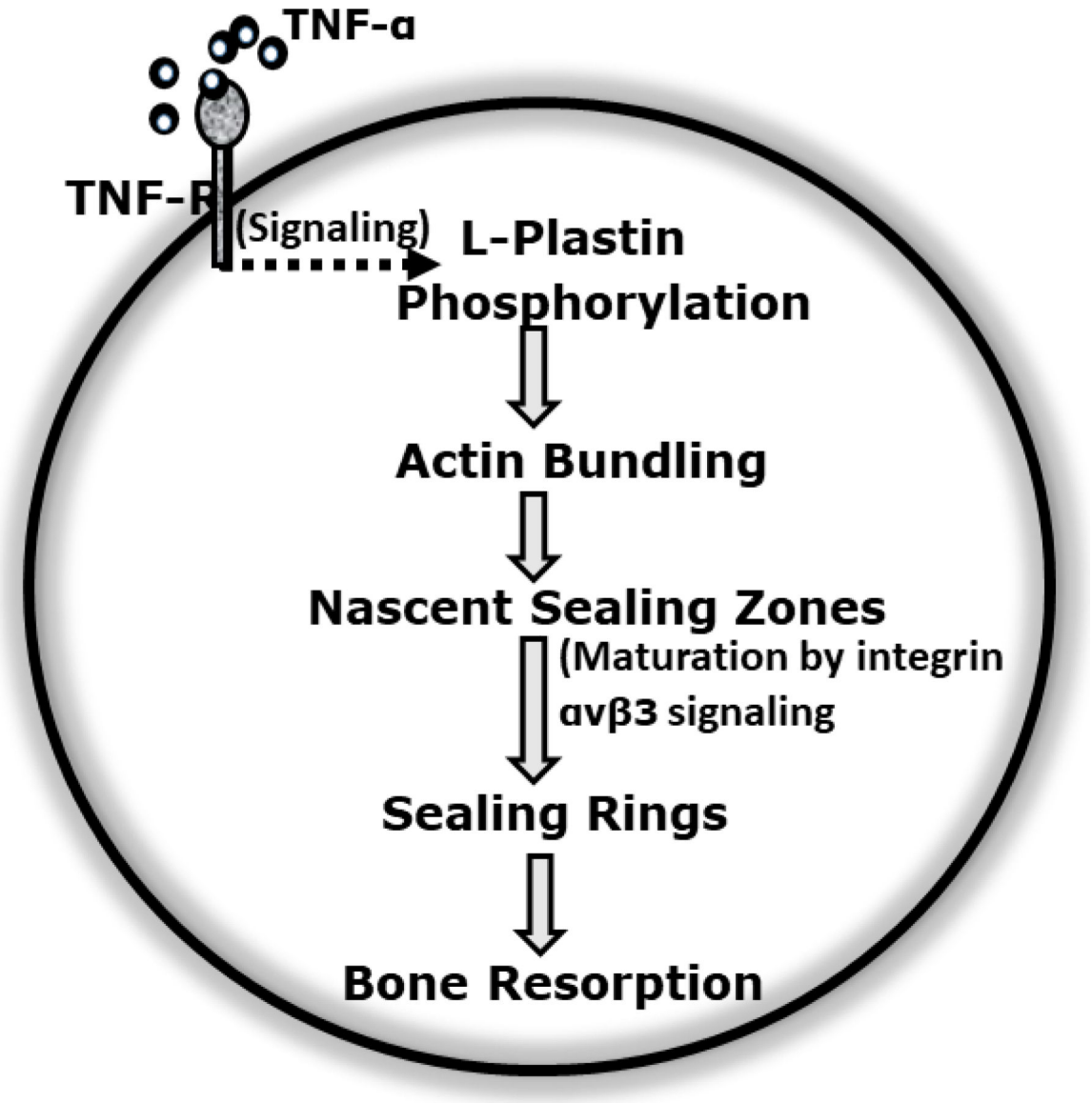

Figure 7:
Schematic representation of the regulation of NSZ formation by TNF- α or RANKL signaling and maturation of NSZs to sealing rings by αvβ3 signaling.